Research Article

S. Vinod Selvaganesh*, P. Dhanasekaran, and Santoshkumar D. Bhat*

TiO_2-nanowire/MWCNT composite with enhanced performance and durability for polymer electrolyte fuel cells

https://doi.org/10.1515/eetech-2017-0002
Received Feb 07, 2017; accepted Oct 08, 2017

Abstract: Durability is a major issue and has been the growing focus of research for the commercialization of polymer electrolyte fuel cells (PEFCs). Corrosion of carbon support is a key parameter as it triggers the Pt catalyst degradation and affects cell performance, which in turn affects the longevity of the cells. Herein, we describe a hybrid composite support of TiO_2-nanowires and Multi-walled carbon nanotubes (MWCNTs) that offers resistance to corrosion under stressful operating conditions. Titania nanowires which have been shown to be more efficient and catalytically active than spherically shaped TiO_2. TiO_2-MWCNT composites are prepared through a hydrothermal method, followed by Pt deposition using a polyol method. Crystal structure, morphology, and oxidation state are examined through various characterization techniques. Electrochemical performance of TiO_2-nanowire/MWCNT composite-supported Pt at various ratios of TiO_2/MWCNT is assessed in PEFCs. Pt on support with optimum composition of TiO_2-nanowires to MWCNTs exhibits fuel cell performance superior to Pt on MWCNTs. Accelerated stress testing (AST) between 1 and 1.5 V reveals that the designed catalyst on nanocomposite support possesses superior electrochemical activity and shows only 16% loss in catalytic activity in relation to 35% for Pt/MWCNTs even after 6000 potential cycles. Subsequently, the samples were characterized after AST to correlate the loss in fuel cell performance

Keywords: Accelerated stress test (AST); Support corrosion; Titania nanowires-MWCNT composite

1 Introduction

In current energy crisis scenario, polymer electrolyte fuel cells (PEFCs) are considered promising systems for hydrogen energy conversion and sustainable energy application suited for both stationary and portable applications. The present focus of the investigation primarily stresses durability and cost, which are inter-related [1]. In order to improve the durability of PEFCs, an understanding of the degradation of catalyst, support and their mitigation strategies is crucial. Carbon-based supports are the conventional choice for platinum (Pt) electrocatalyst in PEFCs. However, the carbon support corrosion, particularly in the cathode during start-up and shut-down remains a bottleneck towards the sustainable long-term stability of PEFCs [3, 4].

In this regard, focus has been shifted towards corrosion resistant support materials that can also stabilize the Pt electrocatalysts in PEFCs [5–10]. One such approach is applying more graphitic carbon-like carbon nanotubes (CNTs), carbon nanofibers (CNFs) and graphene as supports for PEFCs [11–14]. Multi-walled carbon nanotubes (MWCNTs) are particularly attractive as a catalyst support for PEFC applications owing to their unique mechanical, electrical and thermal stability [15–20]. However, aggregation of nanotubes and problems associated with dispersion of Pt electrocatalyst are a challenging task that renders them less desirable [20, 21]. The second approach is use of stable transition metal-oxides as catalyst-supports. In this regard, TiO_2 possesses superior stability in highly corrosive environments and exhibits good catalytic stability making it certainly interesting [21, 22]. However, a substantial loss in the performance of PEFCs has been made particularly due to its lower conductivity [23, 24]. To overcome this drawback, a hybrid nanocomposite consisting

***Corresponding Author: S. Vinod Selvaganesh:** CSIR-Central Electrochemical Research Institute-Madras Unit, CSIR Madras Complex, Chennai - 600 113 India; Email: svsganesh.dr@gmail.com
***Corresponding Author: Santoshkumar D. Bhat:** CSIR-Central Electrochemical Research Institute-Madras Unit, CSIR Madras Complex, Chennai - 600 113 India; Email: sdbhat@cecri.res.in

P. Dhanasekaran: CSIR-Central Electrochemical Research Institute-Madras Unit, CSIR Madras Complex, Chennai - 600 113 India; Email: dhanascient@gmail.com

of TiO_2 and highly conducting carbon nanotubes (CNTs), that can have high activity and durability through its interaction with Pt, is promising for PEFC applications. According to literature reports, TiO_2/MWCNT nanocomposites are demonstrated to have improved photo-catalytic activity [25–27]. In addition, nanocomposites comprised of TiO_2/MWCNTs are shown to have higher efficiency in solar cells [28]. According to literature reports, titania nanowires have been shown to be more efficient and catalytically active than TiO_2 spherical nanoparticles in various applications [29, 30]. According to a report by Hardcastle, efficiency of TiO_2 nanotubes is higher towards photocatalytic splitting of water than of spherically shaped TiO_2 [31]. Song *et al.* reported that titania nanotubes prepared from polycrystalline TiO_2 have more interesting and unique properties than the latter [32]. It has been reported that the one-dimensional TiO_2 has larger surface area than the TiO_2 nanoparticles, which is essential, particularly in heterogeneous catalysis [32–34]. Shen *et al.* investigated TiO_2/MWCNTs based nanocomposites for usage in lithium-ion battery and this nanocomposite seems to be ideal for fast and efficient lithium storage [35]. De Luca *et al.* have explored the sensing characteristics of Pt/TiO_2/MWCNTs composites and found that the synergistic action between Pt, TiO_2 and MWCNTs plays a key role in fast response of this catalyst for hydrogen sensing [36].

In the literature, a few studies are available for Pt supported on TiO_2 nanostructures, MWCNT and their composites as electrocatalyst for PEFCs with appreciable electrochemical activity [21, 37–40]. Our previous study reported the enhanced electrocatalytic acitivity towards ORR using a Pt/TiO_2:TiN electrocatalyst [40]. Xia *et al.* prepared CNT@TiO_2 structures composed of TiO_2 nanosheets grafted on the CNT backbone as the support [21]. Ocampo *et al.* prepared Pt-TiO_2-CNT through a metal-organic chemical vapor deposition (MOCVD) process and the results showed that the Pt-TiO_2-CNT composites displayed higher Pt activity than the Pt-TiO_2 catalysts [38]. In addition, the above-mentioned catalysts were also evaluated for methanol and ethanol electro-oxidation [41–43]. The studies did not demonstrate actual fuel cell performance and stability during long-term operation in fuel cell mode. Also, it is imperative and vital to study various composition ratios of TiO_2 nanowire to MWCNT, which is expected to tailor its properties towards activity and durability of Pt in PEFCs. Hence, we envisage the use of optimum ratio of TiO_2 to MWCNTs as support for Pt in PEFCs. Herein, we describe a hybrid composite based on optimum ratio of TiO_2 nanowires and MWCNTs that can disentangle the setbacks associated with Pt dispersion and the reduced conductivity of TiO_2. Besides, hybrid nanocomposites of TiO_2-CNT could provide added advantages, pertaining to the unique electronic structure, large surface area, enhanced stability of CNTs, and increased acid stability, corrosion resistance and improved catalytic activity associated with TiO_2 [44]. In this study, a hybrid composite of TiO_2 nanowires (TNW) and MWCNTs composite (TWCNTs) for fuel cell operation is demonstrated. Various compositions of TWCNT (C to Ti ratio) are prepared through a hydrothermal method. Pt is deposited on TWCNT by using a polyol method. Morphology, microstructural properties, surface compositions and oxidation state of electrocatalyst samples are evaluated using X-ray diffraction (XRD), field emission-scanning electron microscopy (FE-SEM), transmission electron microscopy (TEM) and X-ray photoelectron spectroscopy (XPS). Cyclic voltammetry and cell polarization studies are carried out in order to assess the influence of the supports on the overall performance. An accelerated stress test (AST) protocol is employed to analyze the stability of the supports in actual fuel cell environment under stringent operating conditions. The tailored electrocatalyst is demonstrated to have higher performance in PEFCs and to be stable up to 6000 cycles between 1 and 1.5 V. After the AST, the catalytic activity and physical properties of Pt/TWCNTs are compared with those of Pt/TNW and Pt/MWCNT.

2 Experimental

2.1 Preparation of titania nanowires

Titania nanowires were prepared by hydrothermal method. In brief, about 3 g of Degussa TiO_2 [P-25] procured from Aldrich Chemicals was dispersed in 100 ml of 10 M KOH by ultrasonication for 20 min and stirred for 1 h to get a homogenous suspension. Further, this suspension was transferred to a Teflon-lined autoclave and heat-treated at 200°C for 48 h. Finally, titania nanowires (TNW) were obtained after cooling to room temperature and filtration, washing with diluted HCl, de-ionised water and methanol. The obtained TNW samples were dried at 70°C for 12 h. Formation of titania nanowires was confirmed by FE-SEM measurements discussed in the later sections.

2.2 Surface treatment of multi-walled carbon nanotubes (MWCNT)

Prior to the formation of nanocomposites, the MWCNT (outer diameter 10-30 nm) (Aldrich chemicals) were sur-

face treated according to the procedure reported elsewhere [45]. In brief, an acid mixture containing 1:1 ratio of conc. HNO_3 and conc. H_2SO_4 was prepared and 1 g of MWCNT was suspended. Further the acid mixture containing MWCNTs was ultrasonicated for about 40 min and stirred vigorously for 2 h at 80°C. Finally, MWCNT were separated after repeated washing with de-ionized water and dried subsequently at 80°C for 8 h.

2.3 Preparation of TWCNTs nanocomposite

TWCNTs nanocomposite was prepared from as-synthesised TiO_2 nanowires and surface-treated MWCNTs by a hydrothermal method. In brief, the required amount of TiO_2 nanowires and MWCNTs was dispersed in isopropyl alcohol (IPA)-water mixture under ultrasonication for 20 min followed by stirring for 1 h. This suspension is further transferred to a Teflon-lined autoclave and heat-treated at 150°C for 6 h. The nanocomposites were purified through repeated washing with excess of deionized water followed by drying at 80°C for 12 h. Various ratios of TWCNTs nanocomposite in terms of C to Ti weight percentage such as 1:1, 2:1 and 3:1 were prepared by the above method and labelled as TWCNT-1, TWCNT-2 and TWCNT-3 respectively.

2.4 Deposition of Pt nanoparticles on MWCNTs and TWCNT nanocomposite

Pt electrocatalyst with a composition of 30 wt.% of Pt on TWCNT-1 was prepared by a polyol method. In a typical experiment, 120 mg TWCNT-1 was dispersed in 2:1 volume ratio of ethylene glycol-water mixture. Approximately, 215 mg $H_2PtCl_6{\cdot}6H_2O$ (Aldrich Chemicals) was added to the above solution dropwise under constant stirring, the solution sonicated for 30 min, the pH was adjusted to 13 by the addition of sodium hydroxide. Further, the solution was refluxed in a round bottom flask at 140°C for 6 h. Finally, Pt-deposited on TWCNT-1 (Pt/TWCNT-1) was separated from ethylene glycol solution after repeated washing with copious amounts of Millipore water followed by ethanol and drying in a hot air oven at 80°C for 12 h. Similarly, the above method was followed for the preparation of Pt/TNW, Pt/MWCNT and Pt/TWCNTs.

2.5 Fabrication and evaluation of membrane electrode assemblies (MEAs)

MEAs were fabricated following a proprietary protocol reported in our previous work [46]. To sum up, a Toray carbon paper (TGP-H-120) of 0.35 mm thickness with 15 wt% Teflonization was used as the backing layer. For gas-diffusion layer, Vulcan XC72R carbon suspended in cyclohexane and ultrasonicated in a water bath for 40 min with 15 wt% Teflon suspension was brush-coated on to the Teflonized carbon paper and heat-treated at 350°C for 30 min.

To prepare the catalyst layer, the required amount of the catalyst (Pt/C for anode and Pt/TNW, Pt/MWCNT or Pt/TWCNTs for cathode) was suspended in IPA and the mixture was ultrasonicated in a water bath. Further, 7 and 30 wt.% of Nafion® (Dupont) ionomer, respectively, was added to the anode and cathode slurry with continuous sonication for 1 h. The resultant suspension was coated onto the gas-diffusion layer. Both anode and cathode contained a platinum loading of 0.2 mg cm^{-2} (active area 25 cm^2) that was kept constant in all the MEAs. Finally, MEAs were obtained by hot pressing the cathode and anode on either side of a pre-treated Nafion-212 membrane at 60 kg cm^{-2} at 130°C for 2 min. MEAs were evaluated using a conventional 25 cm^2 fuel cell fixture with parallel serpentine flow field setup procured from M/s Fuel Cell Technologies Inc., US. Prior to measurement of polarization data, the cells were equilibrated at constant potential at 60°C. The polarization data were recorded at varying load current-densities at 60°C with the recommended stoichiometry of hydrogen (1.2) and oxygen (3) under ambient pressure on BioLogic Science Instruments Corporation (FCT150S), France.

2.6 Accelerated stress test (AST)

AST was carried-out following a detailed standard durability testing protocol [47]. In brief, AST was carried-out by potential cycling the cathode of the PEFC between 1 and 1.5 V with respect to the dynamic hydrogen electrode (DHE) using a potentiostat (Autolab-PGSTAT 30). The test was conducted at a cell temperature of 80°C with humidified hydrogen at a flow rate of 1.2 stoichiometry at 1 A cm^{-2} and 100 ml min^{-1} of nitrogen to cathode, respectively. Cell polarization and CV for measuring ESA were conducted at frequent intervals of AST.

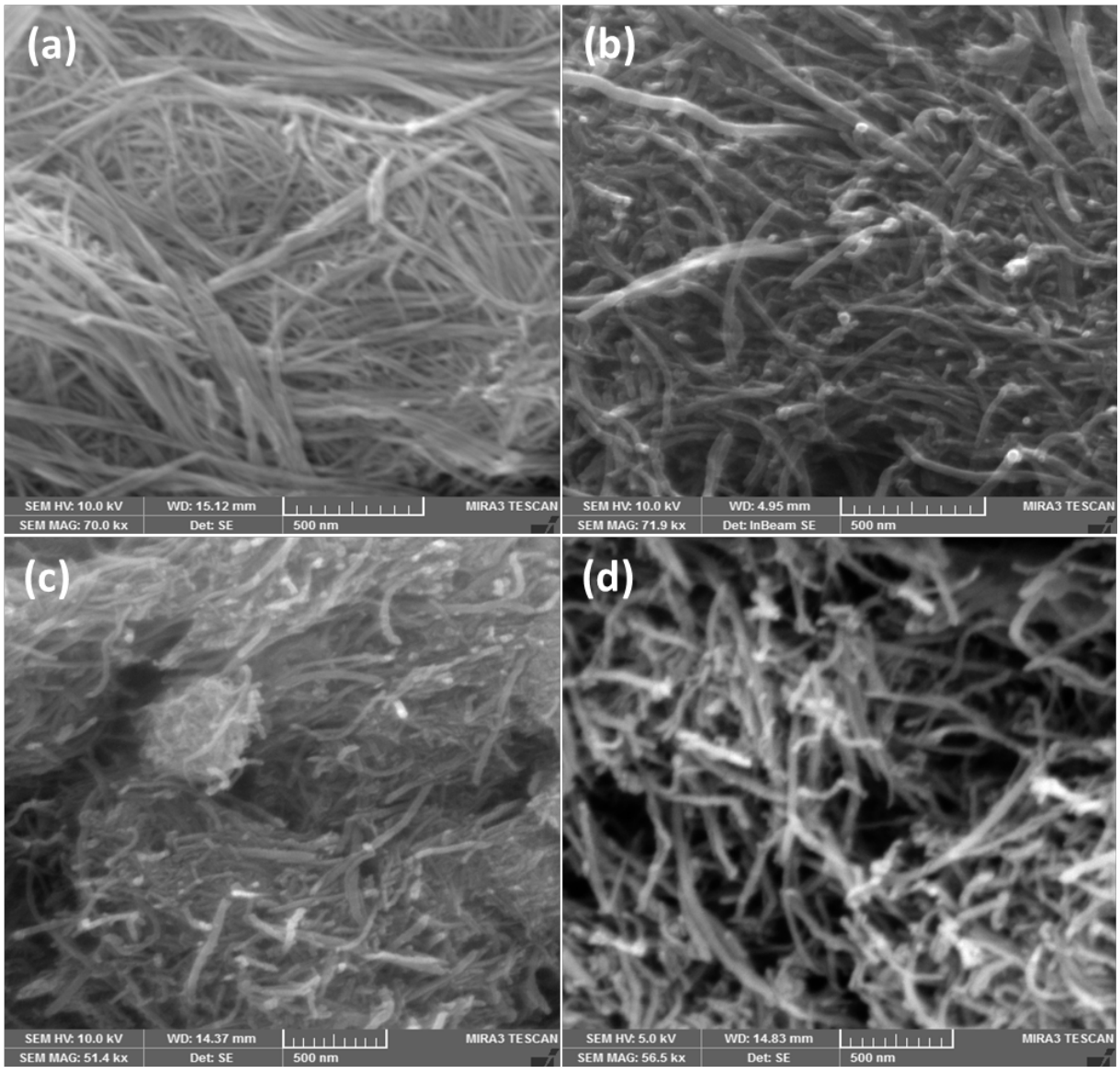

Figure 1: FE-SEM images of (a) TNW, (b) MWCNT, (c) TWCNT-3 and (d) TWCNT-2.

2.7 Physical characterization

Powder X-ray diffraction (PXRD) studies were conducted on Philips X'Pert diffractometer using CuKα radiation (λ = 1.5406 Å) to analyze the change in crystallinity and crystallite size of Pt in Pt/TNW, Pt/ MWCNT and Pt/TWCNTs. X-ray photoelectron spectroscopy (XPS) studies were conducted to analyze the oxidation states of the elements using Omicron nanotechnology instrument, Germany. The morphologies, average particle size of Pt and surface atomic compositions for various electrocatalyst were examined using TESCAN MIRA 3 field emission-scanning electron microscope (FE-SEM) with dispersive X-ray spectrometry (EDX), transmission electron microscopy (TEM) and high resolution-transmission electron microscopy (HR-TEM) using Tecnai G20 and G30, respectively.

3 Results and Discussion

The surface morphology of the hybrid composites for various electrocatalysts has been examined by FE-SEM. Figure 1 (a-d) shows FE-SEM images for MWCNT, TNW and TWCNT nanocomposite electrocatalysts. Figure 1 reveals the one-dimensional nanowire structure of titania prepared through hydrothermal method (a) and MWCNTs (b). Figure 1 (c & d) shows images of TWCNT-3 and 2, wherein titania nanowires are seen entangled with MWCNTs to give

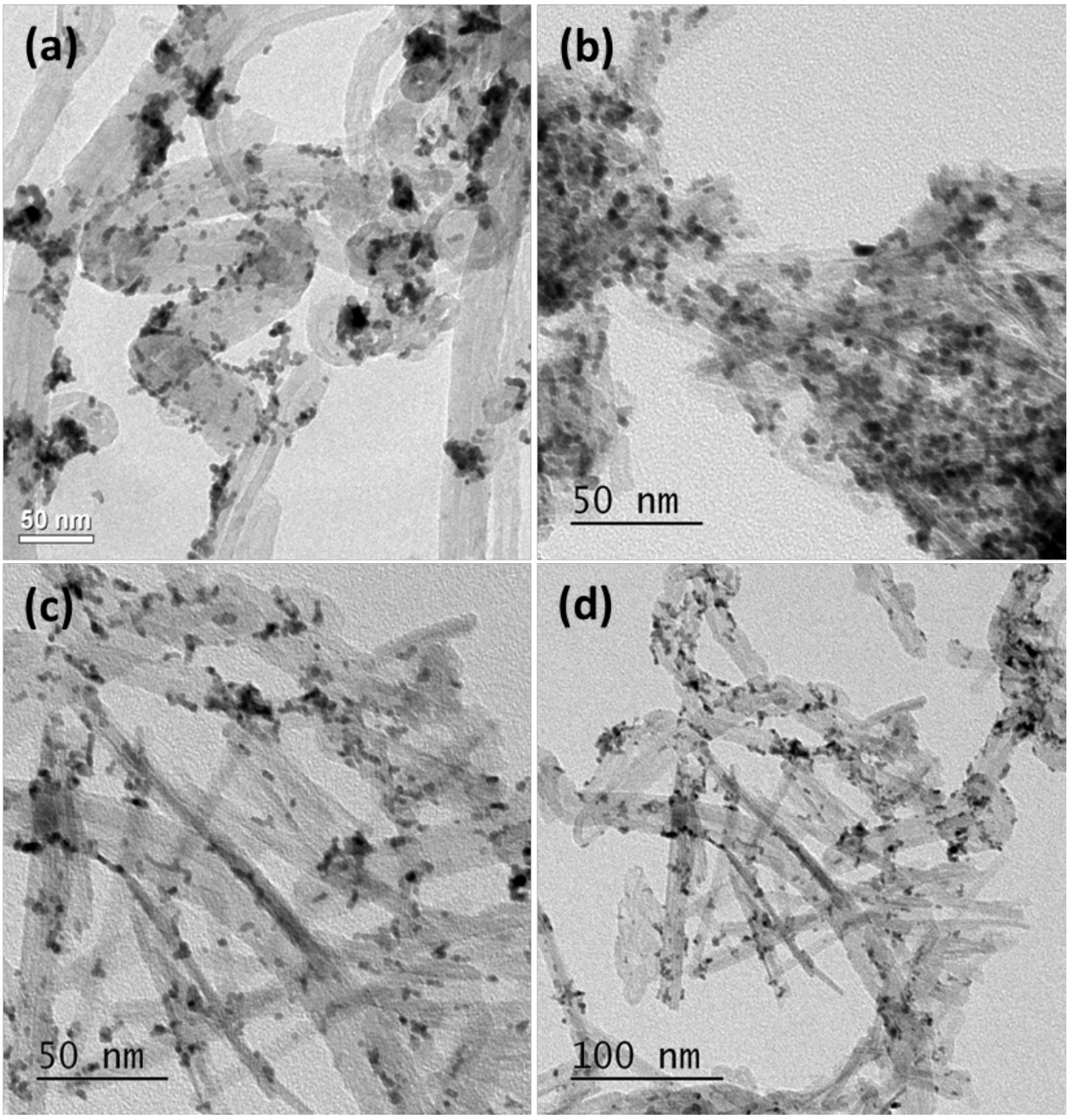

Figure 2: HR-TEM micrographs of (a) Pt/MWCNT, (b) Pt/TNW, (c & d) Pt/TWCNT-2 at different magnifications.

an intertwined structure of TWCNT nanocomposite. In addition, EDX was taken for Pt deposited on MWCNT, TNW and TWCNT nanocomposite electrocatalysts. EDX result clearly shows Pt content in all the electrocatalyst to be 30-32 wt.% and no other impurities were detected. To further examine the Pt particle size, distribution and structural morphology, HR-TEM images were taken for various electrocatalysts. Figure 2 (a-d) shows the HR-TEM images for Pt/MWCNT, Pt/TNW and Pt/TWCNT electrocatalysts. In the case of Pt/MWCNT, the Pt nanoparticles are distributed evenly with slight agglomeration as shown in Figure 2 (a). Whereas, in the case of Pt/TNW, fairly uniform distribution of Pt nanoparticles is seen and the nanowires are closely packed like bundles as shown in Figure 2 (b). HR-TEM micrographs for Pt/TWCNT-2 nanocomposite as given in Figure 2 (c & d) reveal the entangled nanowire-nanotube structure with fairly uniform distribution of smaller sized Pt nanoparticles. The Pt particle size for Pt/MWCNT, Pt/TNW and Pt/TWCNTs nanocomposite is observed to be on the order of 2-6 nm with majority of the particles to be 4 nm. HR-TEM micrographs for Pt/TWCNT-1, 2 and 3 are also given in the Supporting Information (Fig-

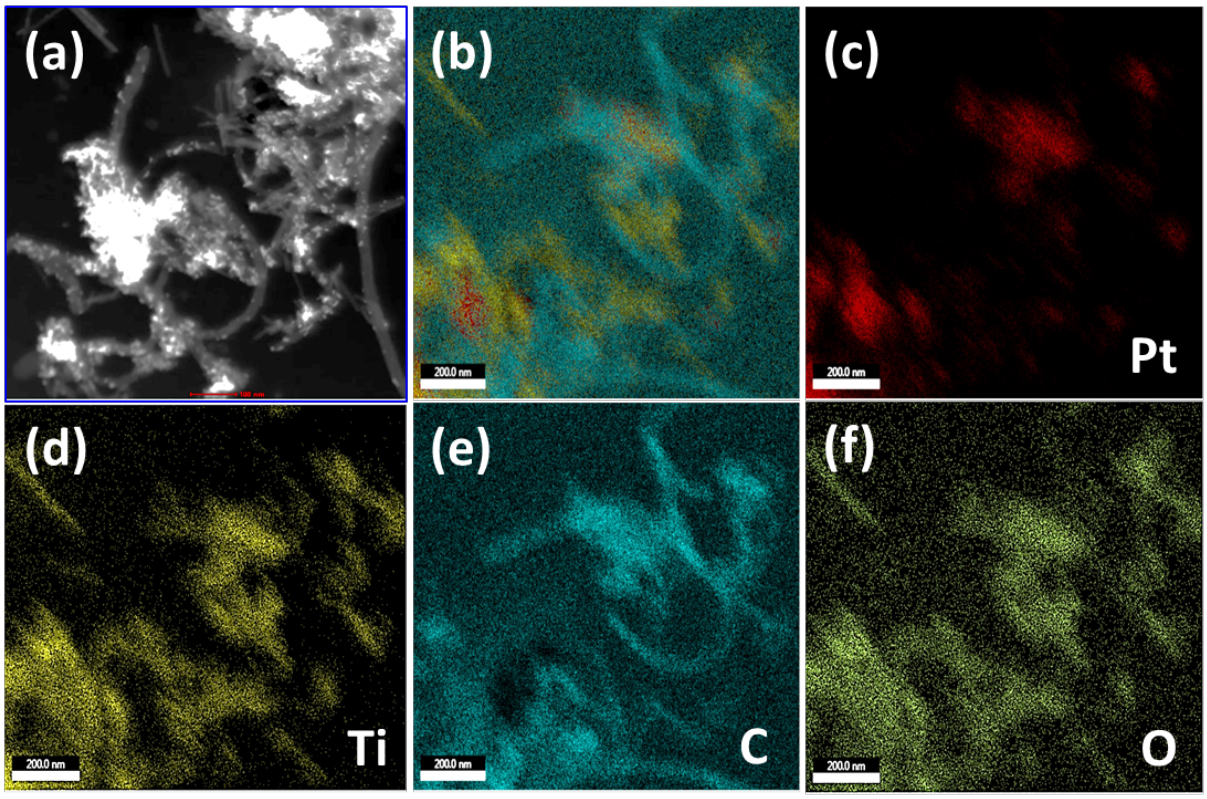

Figure 3: (a-f) Typical STEM and elemental mapping for Pt/TWCNT-2; (a) STEM, (b) Overall mapping, (c) mapping for Pt, (d) Ti, (e) C and (f) O.

ure 1S (a-c)). Histogram showing the Pt particle size distribution for Pt/MWCNT, Pt/TNW and Pt/TWCNT-2 nanocomposite is given in Supporting Information (Figure 2S). The typical STEM and elemental mapping for Pt/TWCNT-2 in Figure 3 (a-f) clearly show TiO_2 nanowires getting composited with the MWCNTs forming a perfect intertwined structure with Pt deposited on TWCNT-2.

PXRD patterns for Pt deposited on MWCNT, TNW and various compositions of TWCNT nanocomposite are given in Figure 4. PXRD pattern for TiO_2 nanowires at 25.26, 48.35 and 68.78° corresponds to the lattice planes (101), (200) and (116) of anatase TiO_2, respectively. Similarly, TWCNT nanocomposites also show typical peaks for (101) and (200) lattice planes of anatase TiO_2. In addition, the peak at 26° corresponding to C (002) plane is seen overlapping with the (101) plane peak of titania. Pt/MWCNT, Pt/TNW and Pt/TWCNT electrocatalysts show broad peaks at 39.8, 46.4 and 67.6° corresponding to (111), (200) and (220) lattice planes, confirming the face-centered cubic (fcc) structure of Pt metal particles (JCPDS no. 87-0647). The platinum crystallite size is calculated from full-width-at-half-maximum (FWHM) value for the (111) peak using Scherrer equation [46]. The average Pt crystallite sizes in Pt/TNW, Pt/MWCNT and Pt/TWCNTs electrocatalysts are furnished in Table 1S in the Supporting Information. It is observed that the Pt crystallite size remains almost the same for Pt/TWCNT-1, 2 and Pt/TNW. The Pt crystallite size measured with XRD is in agreement with that observed in HR-TEM micrographs.

Figure 5 (a and b) depicts the XPS survey spectra of Pt/TNW and Pt/TWCNTs nanocomposite electrocatalysts. The XPS survey spectra for Pt/TNW and Pt/TWCNT-2 clearly reveal the presence of the expected elements with no other impurities. Figure 5 (c and d) shows the Ti2p binding energy level for Pt/TNW and Pt/TWCNT-2 electrocatalysts. The binding energy doublet peaks at 464.2 and 458.4 eV for Pt/TNW correspond to the Ti 2p1/2 and Ti 2p3/2 asymmetric spin orbit levels, which confirm Ti to be present in +4 oxidation state. Whereas, in the case of TWCNT-2, a small shift is observed in the binding energy at 464.5 and 458.8 eV, which is mainly due to the strong interaction between titania and MWCNT. Figure 5 (e and f) shows the deconvoluted O1s spectra for Pt/TNW and Pt/TWCNTs nanocomposite. The O1s spectrum for Pt/TNW shows three different peaks at 530.4, 531.4 and 532.4 eV assigned to the lattice oxygen, surface hydroxyl groups and water molecules in TiO_2, respectively. However, in the case of Pt/TWCNTs nanocomposite, apart from the above three

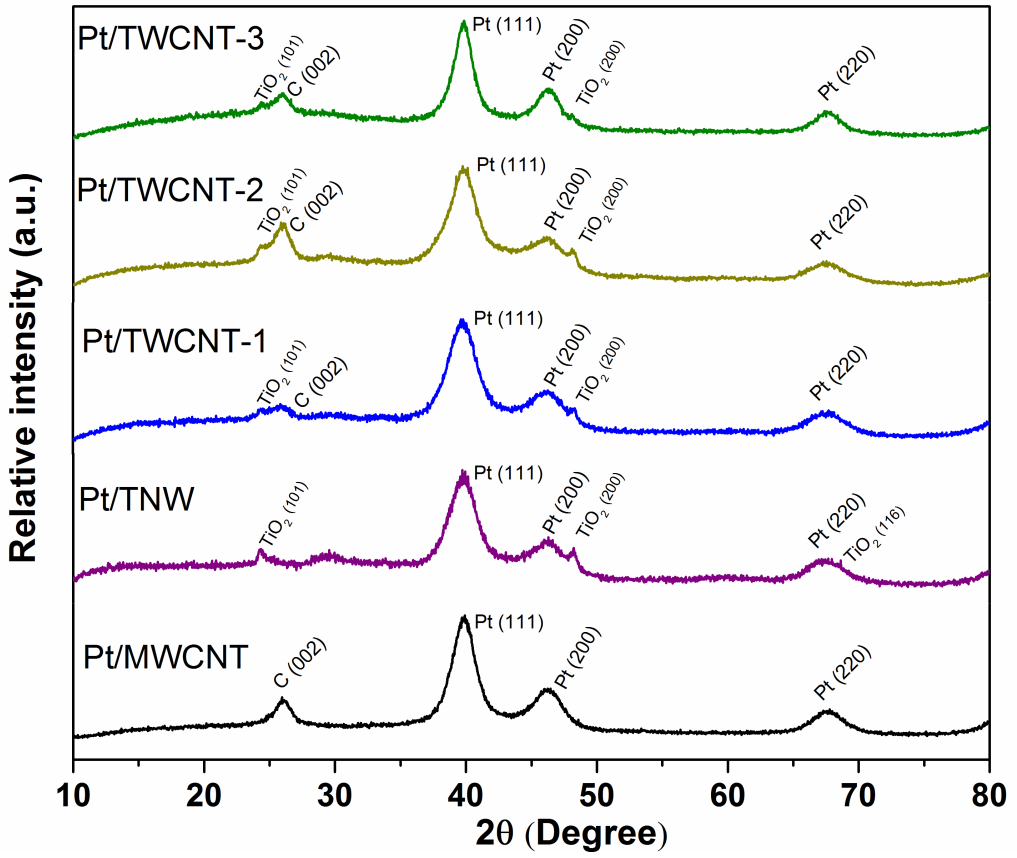

Figure 4: Powder XRD pattern for Pt/MWCNT, Pt/TNW and various nanocomposites supported Pt (Pt/TWCNT).

peaks, an additional peak at 533.2 eV corresponds to the O-C bond. This clearly confirms the interaction between the TiO_2 nanowires and MWCNTs through Ti-O-C bond [48].

From the deconvoluted spectra of the 4f region, it can be seen that Pt (4f) for Pt/MWCNT and Pt/TWCNT-2 electrocatalysts consist of three pairs of doublet peaks as shown in Figure 6 (a-b) which are attributed to Pt^0, Pt^{II} and Pt^{IV} oxidation state. Figure 6 (a) depicts the Pt 4f binding energy peaks at 74.7 and 71.4 eV corresponding to Pt 4f 5/2 and 4f 7/2 orbital swhich is attributed to metallic state of Pt for Pt/MWCNT in good agreement with literature reports [49, 50]. However, as compared to Pt/MWCNT (Figure 6 (a)) of Pt 4f level, the Pt doublet metallic peaks are shifted towards higher energy levels in case of Pt/TWCNT as shown in Figure 6 (b). This may be due to the strong metal-support interaction between Pt and titania nanowires which modifies the electronic and catalytic properties of Pt. The relative percentages of Pt^0, Pt^{II} and Pt^{IV} for Pt/TWCNTs are observed to be 78, 13 and 9% respectively, which is very similar to that of Pt/MWCNT and Pt/TNW.

The performance data for PEFCs with Pt/MWCNT, Pt/TNW and Pt/TWCNTs employed as cathode catalysts are presented in Figure 7 (a). From the polarization curves, it is clear that Pt/TWCNT nanocomposites, particularly Pt/TWCNT-1 and 2 composite electrocatalyst exhibit better performance followed by Pt/MWCNT and Pt/TNW in the entire polarization region with the order of performance being Pt/TWCNT-2 > Pt/TWCNT-1 > Pt/MWCNT > Pt/TWCNT-3 > Pt/TNW. The PEFC with Pt/TWCNT-2 shows a current density of 810 mA cm^{-2} at 0.6 V in relation to Pt/MWCNT and Pt/TNW wherein current density of 600 and 350 mA cm^{-2} is seen, respectively. The unique electronic structure of MWCNTs helps enhancing the catalytic activity of the Pt electrocatalyst in addition to its enhanced ballistic electron transport. Besides, the titania nanowires show enhanced electrocatalytic activity by their interaction with Pt nanoparticles [36, 48, 51]. Together, the combination of titania nanowires along with MWCNTs enhanced the catalytic activity of Pt through their interaction and improved the fuel cell performance. MWCNTs as support provides mechanical integrity to the support structure, whereas titania nanowires are proven to be active towards catalysis [52, 53]. Literature report also shows titania in nanowire/nanorod form to be catalytically more active than in spherical form [33]. The MWCNTs in the interconnected twinned-structure also act as charge-carriers

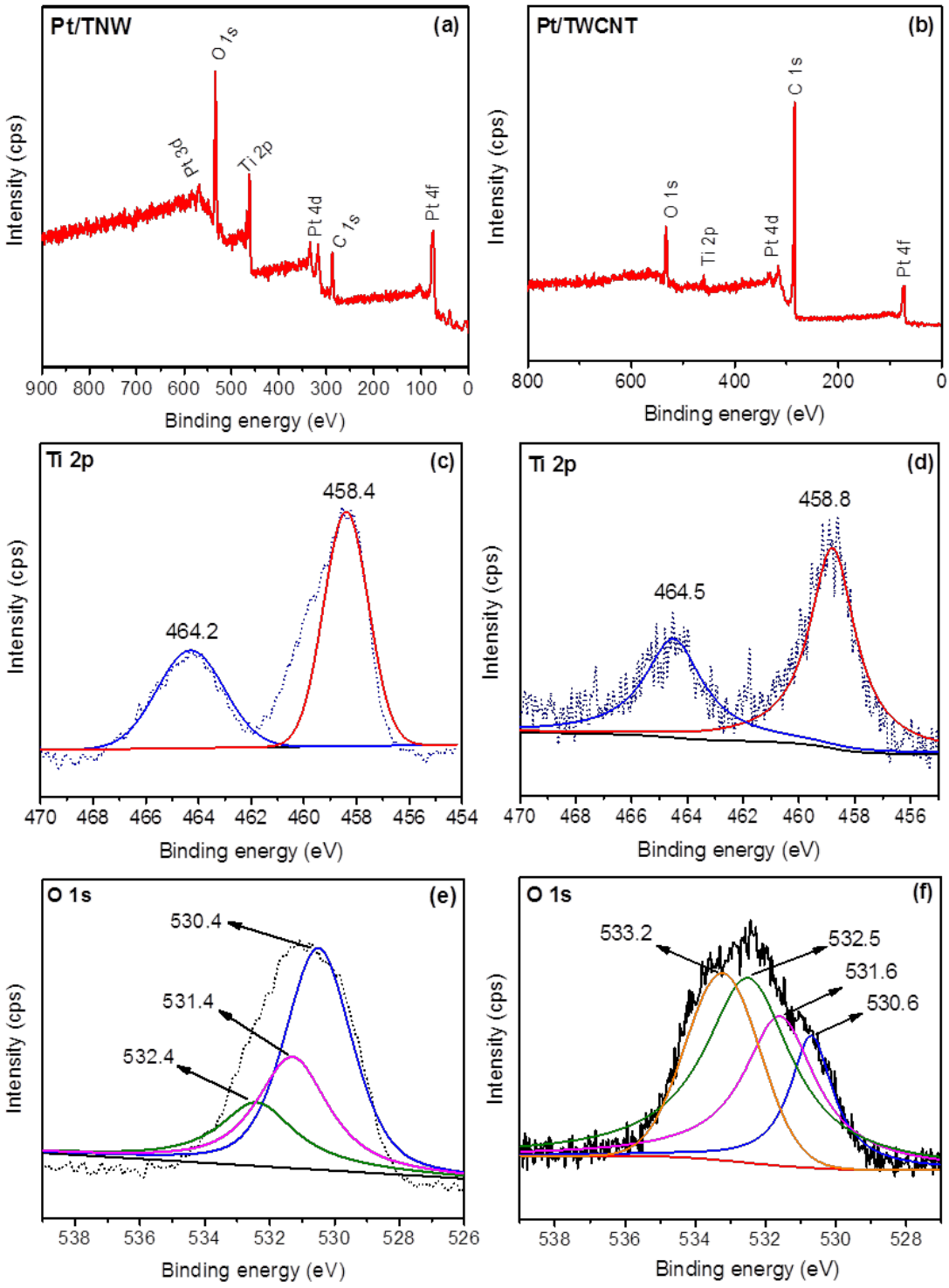

Figure 5: XPS (a & b) survey spectra for Pt/TNW and Pt/TWCNT-2, (c & d) deconvoluted spectra of Ti 2p state for Pt/TNW and Pt/TWCNT-2 and (e & f) O 1s for Pt/TNW and Pt/TWCNT-2.

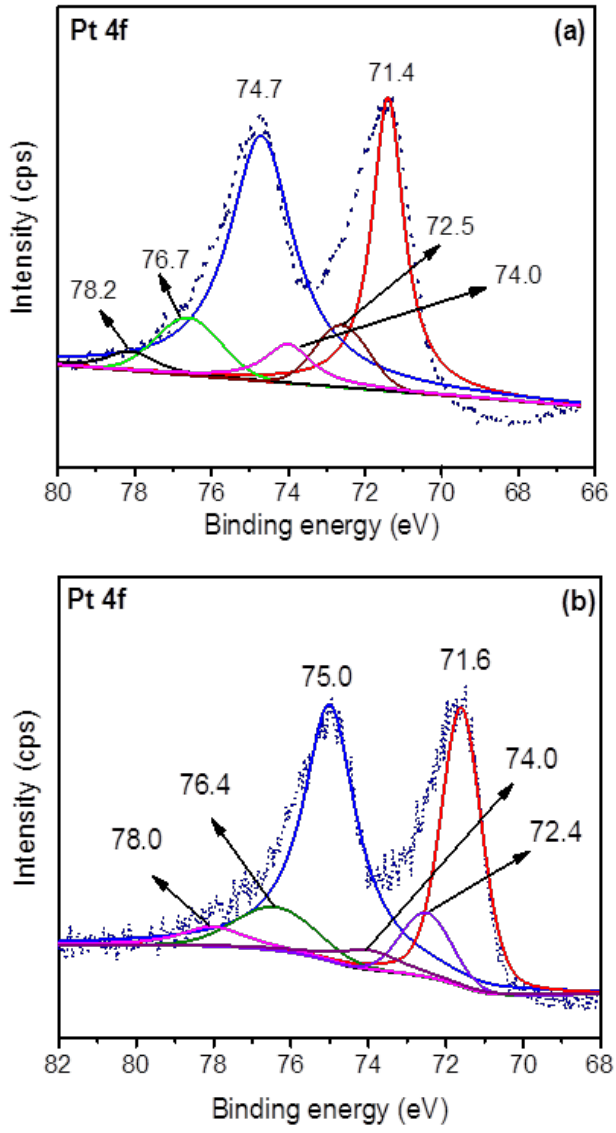

Figure 6: XPS deconvoluted spectra of Pt 4f state for (a) Pt/MWCNT and (b) Pt/TWCNT-2.

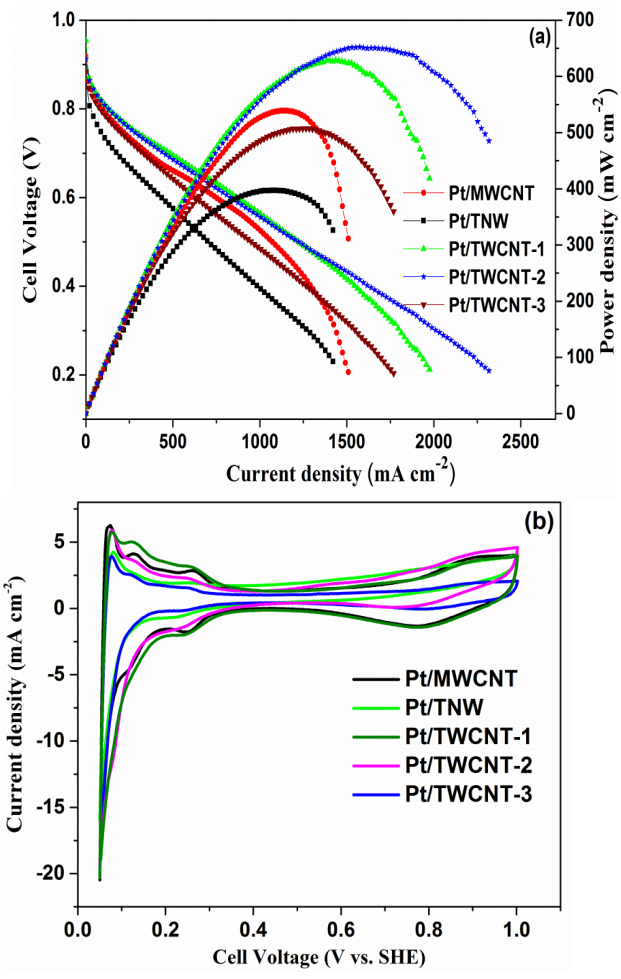

Figure 7: (a) Comparative steady-state polarization curves and (b) Comparative CV recorded for Pt/TNW, Pt/MWCNT and Pt/TWCNTs.

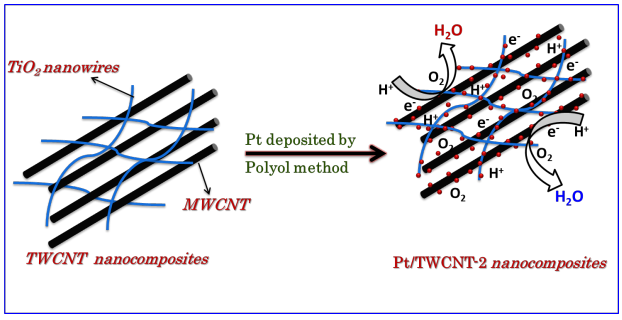

Scheme 1: Representation of TiO_2 nanowires on to the MWCNT surface followed by the deposition of Pt and ORR surface mechanism on the as formed Pt/TWCNT-2 nanocomposite.

and compensate for the conductivity loss with titania. A graphic representation illustrating the entangled structure of titania nanowires and MWCNTs followed by the deposition of Pt nanoparticles is presented in Scheme 1. The illustration of the one-dimensional local arrangement of titania nanowires and MWCNTs is based on the inference from structural investigations.

It is expected that the increased TiO_2 content in the Pt/TWCNT-1 has a lot of TiO_2 nanowires aggregated on the MWCNT surface. This may be the reason behind the slightly reduced performance at high current densities due to sluggish charge transport across TiO_2 to MWCNT assembly. In the case of Pt/TWCNT-3, there is a lack of surface coverage of MWCNT by TiO_2 nanowires. This results in the poor distribution of Pt, some of the Pt nanoparticles are attached directly to MWCNTs leading to reduced cell performance. However, Pt/TWCNT-2 shows better performance than other combinations in the entire polarization region. Thus, TiO_2 nanowires to MWCNTs with C-Ti ratio of 2:1 are

found to be optimum for Pt support in PEFCs. This is substantiated in the literature by De Luca *et al.* It is reported that C/Ti ratio in the Pt/TiO2/MWCNT composite plays a vital role in hydrogen detection [36].

To measure the electrochemical surface area (ESA) and to corroborate the electrochemical behaviour with performance, CV studies were carried out, employing Pt/MWCNT, Pt/TNW and Pt/TWCNTs as cathode catalysts. The resultant voltammograms are shown in Figure 7(b). From CV, hydrogen adsorption/desorption (H_{ad}/H_{de}) region in the potential range of 0.05 to 0.4 V (vs. DHE) is observed for all catalysts. The region between 0.4 and 0.65 V corresponds to double layer region and the hump at potentials > 0.65 V is attributed to oxide formation/reduction of Pt. The H_{ad}/H_{de} charge for Pt/TWCNT-1 is higher followed by Pt/TWCNT-2, Pt/MWCNT, Pt/TWCNT-3 and Pt/TNW. From the CV, it is clear that ESA for Pt deposited on TWCNT-1 and -2 are higher in comparison to Pt/TWCNT-3. This is in good agreement with Pt distribution observed in HR-TEM micrographs. In addition, the H_{ad}/H_{de} charges for Pt/TNWs are smaller than for other catalysts, which is attributed to the uniform yet closely packed distribution of Pt nanoparticles which renders some of the Pt in the interior layers unavailable for catalysis. The ESA values estimated from CV for the PEFC cathodes comprising Pt/MWCNT, Pt/TNW, Pt/TWCNT-1, Pt/TWCNT-2 and Pt/TWCNT-3 are 51.8, 30.4, 55.3, 45.59 and 28.3 $m^2 g^{-1}$, respectively. This clearly explains the role of the support and the distribution of Pt nanoparticles and their influence on the ESA and catalytic activity.

Following the evaluation of the initial performance and measurement of ESA values, Pt deposited on MWCNT, TNW and a better performing catalyst among TWCNTs supported Pt (Pt/TWCNT-2) are chosen and subjected to durability studies. Precisely, the PEFCs comprising Pt/MWCNT, Pt/TNW and Pt/TWCNT-2 (henceforth named Pt/TWCNT) cathodes are assessed for stability by potential cycling between 1 and 1.5 V at 80°C as discussed in the experimental part. During the potential transients, the cathode exhaust is connected to the CO_2 sensor.

During potential cycling at higher potentials, there is a predictable performance loss due to independent processes such as oxidation of the support and subsequently Pt nanoparticles being leached-out or agglomerated [54]. During the AST a CO_2 evolution of 70-90 ppm initially is observed for PEFCs with Pt/MWCNT cathode, whereas for Pt/TWCNT only 40-50 ppm is observed for the initial few cycles after which there is no CO_2 evolution. Besides in the case of Pt/TNW up to 1000 cycles, initially 10-30 ppm of CO_2 is observed followed by no CO_2 which may be due to oxidation of carbon in the microporous layers. The increased oxidation rate in the case of MWCNT shows vulnerability of MWCNT in this potential range.

To correlate the loss in ESA of the catalyst and the performance of PEFCs during AST, cyclic voltammetry and cell polarization studies are conducted frequently at short intervals. The performance data for PEFCs comprising Pt/MWCNT, Pt/TNW and Pt/TWCNT as cathode catalysts before and after AST are shown in Figure 3S (SI). It is observed that PEFC with Pt/MWCNT shows a peak power performance of 520 mW cm^{-2} and after 6000 potential cycles of AST, it is drastically reduced to 310 mW cm^{-2}. In the case of Pt/TNW, the initial performance is observed to be 400 mW cm^{-2} and after AST it is observed to be 345 mW cm^{-2}. A similar trend in performance loss was observed for PEFC with Pt/TWCNT which delivered a peak power density of 635 and 545 mW cm^{-2} before and after AST, respectively. The decline in cell performance in the case of Pt/MWCNTs is more as compared to the Pt/TNW and Pt/TWCNTs. Similarly, the deterioration in performance for PEFC with Pt/MWCNT cathode is 40% after 6000 potential cycles in relation to 14 and 16% for Pt/TWCNT and Pt/TNW measured from the loss in peak power performance. In addition, for more clarity the drop in steady-state current density at 0.8, 0.6 and 0.4 V for Pt/MWCNT, Pt/TNW and Pt/TWCNT during AST is given in Figure 8. It is observed that the drop in current density for Pt/MWCNT is more at all three measured voltages. The minimal loss in performance after 6000 potential cycles of AST for Pt/TNW and Pt/TWCNT as cathode catalysts suggests that they are corrosion resistant during fuel-cell operation due to the synergetic nature of TiO_2, resulting in stronger interaction with Pt electrocatalyst.

Interestingly, it is observed from CV curves that there is an increase in the capacitive current for PEFC cathode comprising Pt/MWCNT as cathode electrocatalyst during AST as shown in Figure 4S (SI). This increase in the capacitive current in the CV curve may be attributed to the surface roughening initiated by the surface defects [55, 56]. Similar increase in capacitive current was already observed in our previous study, were carbon corrosion occurred along with increase in capacitance [57]. On the contrary, for the PEFC comprising Pt/TNW and Pt/TWCNT (figure not included) cathode, the increase in capacitance value is comparatively smaller both prior and after AST which indicates stability of MWCNT support against oxidation due to the presence of TiO_2 nanowires. This is in good agreement with the XPS data, which suggest the presence of Ti-O-C interaction providing electrochemical stability in addition to the improvement of catalytic activity. These studies clearly show that titania nanowires and MWCNTs together form a

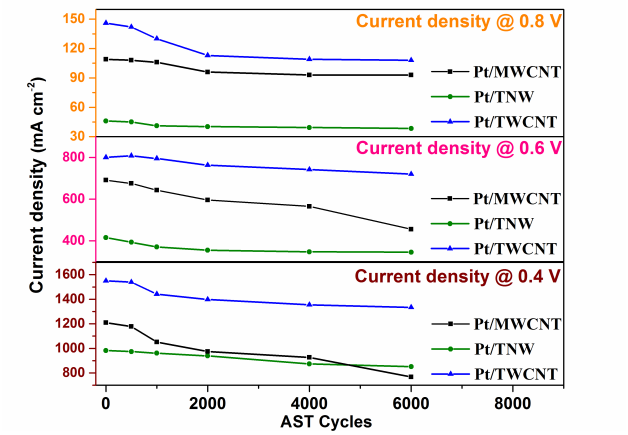

Figure 8: Comparative plot depicting drop in current density for Pt/TNW, Pt/MWCNT and Pt/TWCNT at 0.8, 0.6 and 0.4 V during AST.

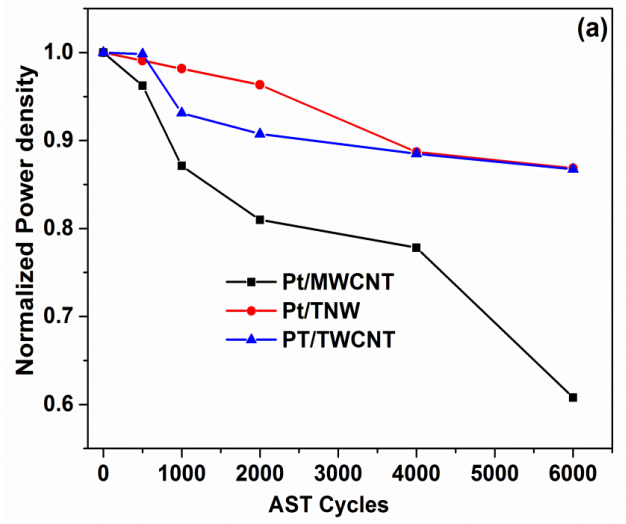

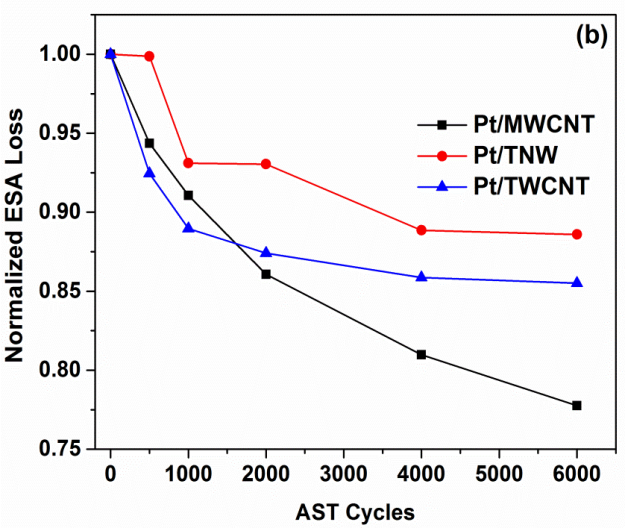

Figure 9: Comparative plot depicting change in (a) steady-state performance and (b) ESA during AST for Pt/ MWCNT and Pt/TWCNT.

stable composite that can demonstrate higher resistance to oxidation.

In order to comprehend the loss in cell performance and ESA for PEFCs with Pt/MWCNT, Pt/TNW and Pt/TWCNT cathodes, the loss in ESA and the steady-state performance values during AST are presented in Figure 9 (a) and (b), respectively. It is observed that for PEFC comprising Pt/MWCNT as cathode electrocatalyst, the cell performance and ESA values though initially stable up to 2000 potential cycles, fall sharply during AST. Whereas, for PEFC comprising Pt/TWCNT as cathode electrocatalyst, the cell performance and ESA values are comparatively stable up to 6000 AST cycles with minimal loss. However, in the case of Pt/TNW, though the initial performance is poor, the stability and resistance to oxidation is higher than that of the other two catalysts. That explains the role of titania nanowires in enhancing the durability of the catalyst as a whole. The partial loss in ESA and performance in the case of Pt/TWCNT may be due to preferential oxidation of MWCNT exposed in some regions of the catalyst layer and followed by loss of Pt active sites. The loss in ESA for Pt/MWCNT is found to be 23% in relation to only 15 and 18% for Pt/TNW, Pt/TWCNT cathode electrocatalysts. Likewise, the drop in performance for PEFCs with Pt/MWCNT, Pt/TNW and Pt/TWCNT as cathode catalysts after AST is 35 and 16%, respectively, after 6000 cycles of AST as measured from the current density at 0.6 V. Hence, the change in steady-state polarization data are akin to the loss in ESA values during AST.

To understand the possible synergistic role of TiO_2 nanowires and MWCNTs in stabilizing the Pt electrocatalyst, the MEAs that were subjected to durability study and also the catalyst collected from the delaminated MEAs were analysed by a set of physical characterization studies. Concisely, in order to ascertain change in crystallinity and morphology for catalysts before and after AST, powder-XRD and TEM studies were carried out. Powder-XRD patterns for Pt/MWCNT, Pt/TNW and Pt/TWCNT electrocatalyst from delaminated MEAs after AST are shown in Figure 5S (SI). The diffraction peaks at $2\theta \approx 26^{\circ}$ corresponding to carbon (002) for both catalysts are broader after AST, which may be due to some amount of graphitic carbon fiber from Toray paper (backing layer). The mean particle size value for Pt particles in Pt/MWCNT is found to increase from 4.3 nm before AST to 7.8 nm after AST. On the other hand, for both Pt/TNW and Pt/TWCNT electrocatalyst, the Pt crystallite size before AST is 3.6 and 4 nm after AST it increases to 5.1 and 5.8 nm, respectively. The uneven increase in Pt crystallite size in Pt/MWCNT is due to the Pt particle agglomeration due to support corrosion. The

above results confirm that the titania nanowires-MWCNTs composite-supported Pt is durable and the nanowire composite support restrains the Pt particle from agglomeration during AST. Subsequently, catalyst samples from the delaminated MEAs were subjected to TEM characterization to analyze any morphology changes of the catalyst and the support during AST. TEM images for Pt/MWCNTs, Pt/TNWs and Pt/TWCNTs catalysts after AST are shown in Figure 6S. It is clearly seen that nanoparticles of Pt are agglomerated with broader particle-size distribution for Pt/MWCNT as compared to Pt/TNW and Pt/TWCNTs.

These data corroborate with corrosion behaviour during AST suggesting that the titania nanowire-based supports and nanocomposites are resistant to oxidation even under highly oxidizing conditions. The role of titania in protecting the Pt nanoparticles is explained in detail by Neophytides *et al.* based on the hypo-hyper-d-inter-electronic bonding and the resulting strong metal-support interaction (SMSI) besides the amelioration of catalytic activity. It is noteworthy that unique electronic structure of MWCNTs helps in enhancing the catalytic activity of the supported metal. In addition, graphitic carbon such as MWCNTs provides mechanical integrity and stability for the highly dispersed metal or metal oxide nanoclusters, resulting in increased stability of Pt/TWCNTs [58, 59]. Thus, the results confirm that optimum composition of TWCNT-2-supported Pt enhanced the cell performance and long-term durability compared to MWCNT-supported Pt.

4 Conclusions

A hybrid support comprising of TiO_2 nanowires (TNW) and MWCNTs composite (TWCNTs) for fuel cell operation is demonstrated. PEFC comprising TWCNT nanocomposite-supported Pt cathode exhibits better cell performance and durability in relation to MWCNT-supported Pt cathode. The deterioration in performance for PEFC with Pt/MWCNT cathode is 35% after 6000 potential cycles in relation to 16% for Pt/TWCNTs, Pt/TNW electrocatalyst. These data corroborate with ESA loss during AST and suggest that the titania nanowire-based supports and nanocomposites are resistant to oxidation even under highly oxidising conditions. The superior stability of the prepared nanowires composite is based on the synergistic role played by the titania nanowires and graphitic MWCNT. Besides, the strong Pt-support interaction is known to play a critical role in the overall stability of Pt/TWCNT nanocomposites electrocatalyst. Thus, a hybrid support comprising TWCNT-supported Pt could possibly overcome the issues related to durability of the catalyst and carbon oxidation support even during stringent PEFC operation conditions.

Acknowledgement: Dr. S. D. Bhat CSIR thanks grant under CSIR-Young Scientist Award (DU-MLP-0090) Scheme. Dr. S. Vinod Selvaganesh and Mr. P. Dhanasekaran gratefully acknowledge CSIR for Research Associateship. We also thank Mr. A. Rathishkumar, Senior Technical Officer, CECRI for his help in TEM characterization.

References

[1] Borup R., Meyers J., Pivovar B., Kim Y.S., Mukundan R., Garland N., Myers D.,Wilson M., Garzon F., Wood D., Zeleney P., More K., Stroh K., Zawodzinski T.,Boncella J., McGrath J.E., Inaba M., Miyatake K., Hori M., Ota K., Ogumi Z.,Miyata S., Nishikata A., Siroma Z., Uchimoto Y., Yasuda K., Kimijima K., IwashitaN., Scientific aspects of Polymer Electrolyte Fuel Cell Durability and-Degradation, Chem. Rev., 2007, 107, 3904-3951.

[2] Stevens D.A., Dahn J.R., Thermal degradation of the support in carbon-supportedplatinum electrocatalysts for PEM fuel cells, Carbon, 2005, 43,179-188.

[3] Reiser C.R., Bregoli L., Pattersin T.W., Yi J.S., Yang J.D., Perry M.L., JarviT.D., A reverse current decay mechanism for fuel cells, Electrochem. Solid-StateLett., 2005, 8, A273-A276

[4] Kangasniemi K.H., Condit D.A., Jarvi T.D., Characterization of VulcanElectrochemically Oxidized under Simulated PEM Fuel Cell Conditions, J. Electrochem. Soc., 2004, 151, E125-E132.

[5] Ferreira P.J., Horn Y.S., Morgan D., Makharia R., Kocha S., Gasteiger H.A.,Instability of Pt/C electrocatalysts in proton exchange membrane fuel cells amechanistic investigation, J. Electrochem. Soc., 2005, 152, A2256-A2271.

[6] Shao Y., Yin G., Gao Y., Understanding and approaches for the durability issuesof Pt-based catalysts for PEM fuel cell, J. Power Sources, 2007, 171,558-566.

[7] Huang S.Y., Ganesan P., Park S., Popov B.N., Development of a titaniumdioxide-supported platinum catalyst with ultrahigh stability for polymerelectrolyte membrane fuel Cell applications. J. Am. Chem. Soc., 2009,131, 13898-13899.

[8] Tintula K.K., Sahu A.K., Shahid A., Pitchumani S., Sridhar P., Shukla A.K.,Mesoporous Carbon and Poly (3,4-ethylenedioxythiophene) Composite as CatalystSupport for Polymer Electrolyte Fuel Cells, J. Electrochem. Soc., 2010,157, B1679-B1685.

[9] Bessel C.A., Laubernds K., Rodriguez N.M., Baker R.T.K., Graphite Nanofibers asan Electrode for Fuel Cell Applications, J. Phys. Chem. B, 2001, 105,1115-1118.

[10] Serp P., Corrias M., Kalck P., Carbon nanotubes and nanofibers in catalysis,Appl. Catal., 2003, 253, 337-358.

[11] Kim K.H., Oh H.S., Kim H., Use of a carbon nanocage as a catalyst support inpolymer electrolyte membrane fuel cells, Electrochem. Commun., 2009, 11,1131-1134.

[12] Iijima S., Helical microtubules of graphitic carbon, Science, 1991,354, 56-58.

[13] Oh H.S., Kim K., Ko Y.J., Kim H., Effect of chemical oxidation of CNFs on theelectrochemical carbon corrosion in polymer elec-

trolyte membrane fuel cells, Int.J. Hydr. Energy, 2010, 35, 701-708.

[14] Ferreira-Aparicio P., Folgado M.A., Daza L., High Surface area graphite asalternative support for proton exchange membrane fuel cell catalysts, J. PowerSources, 2009, 192, 57-62.

[15] Shao Y.Y., Yin G.P., Gao Y.Z., Shi P.F., Durability Study ofPt /C and Pt /CNTs Catalysts under Simulated PEMFuel Cell Conditions, J. Electrochem. Soc., 2006, 153, A1093-A1097.

[16] Shao Y.Y., Yin G.P., Zhang J., Gao Y.Z., Comparative investigation of theresistance to electrochemical oxidation of carbon black and carbon nanotubes inaqueous sulfuric acid solution, Electrochim. Acta, 2006, 51, 5853-5857.

[17] Mohanapriya S., Tintula K.K., Bhat S.D., Pitchumani S., Sridhar P., A novelmulti-walled carbon nanotube (MWNT)-based nanocomposite for PEFC electrodes,Bull. Mater. Sci., 2012, 35, 297-303.

[18] Li L., Xing Y., Electrochemical Durability of Carbon Nanotubes in Noncatalyzedand Catalyzed Oxidations, J. Electrochem. Soc., 2006, 153, A1823-A1828.

[19] Steen E., Prinsloo F.F., Comparison of preparation methods for carbon nanotubessupported iron Fischer–Tropsch catalysts, Catal. Today, 2002, 71,327-334.

[20] Liu Z., Lin X., Lee J.Y., Zhang W., Han M., Gan L.M., Preparation andCharacterization of Platinum-Based Electrocatalysts on Multiwalled CarbonNanotubes for Proton Exchange Membrane Fuel Cells, Langmuir, 2002, 18,4054-4060.

[21] Xia B.Y., Ding S., Wu H.B., Wang X., Wen X., Hierarchically structured Pt/CNT@TiO_2nanocatalysts with ultrahigh stability for low-temperature fuel cells,RSC Advances, 2012, 2, 792–796.

[22] Kraemer S.V., Wikander K., Lindbergh G., Lundblad A., Palmqvist A.E.C.,Evaluation of TiO_2 as catalyst support in Pt-TiO_2/C composite cathodesfor the proton exchange membrane fuel cell. J. Power Sources, 2008, 180,185-190.

[23] Neophytides S.G., Murase K., Zafeiratos S., Papakonstantinou G., Paloukis F.E.,Krstajic N.V., Jaksic M.M., Composite Hypo-Hyper-d-Intermetallic and InterionicPhases as Supported Interactive Electrocatalysts, J. Phys. Chem. B, 2006,110, 3030-3042.

[24] Haarstrick A., Ku O.M., Heinzle E., TiO_2-Assisted Degradation ofEnvironmentally Relevant Organic Compounds in Wastewater Using a Novel FluidizedBed Photoreactor. Environ. Sci. Technol., 1996, 30, 817-824.

[25] Leary R., Westwood A., Carbonaceous nanomaterials for the enhancement ofTiO_2 photocatalysis, Carbon, 2011, 49, 741-772.

[26] Yao Y., Li G., Ciston S., Lueptow R.M., Gray K.A., PhotoreactiveTiO$_2$/carbon nanotube composites: synthesis and reactivity, EnvironmentalScience and Technology, 2008, 42, 4952–4957.

[27] Li Y., Li L., Li C., Chen W., Zeng M., Carbon nanotube/titania compositesprepared by a micro-emulsion method exhibiting improved photocatalytic activity,Applied Catalysis A, 2012, 427-428, 1-7.

[28] Lin K.N., Liou W.J., Yang T.Y., Lin H.M., Lin C.K., Chien S.H., Chen W.C., Wu S.H., Synthesis of hybrid Pt/TiO_2 (anatase)/MWCNTsnanomaterials by a combined sol–gel and polyol process, Diamond and RelatedMaterials, 2009, 18, 312-315.

[29] Wang M., Guo D.J., Li H.L., High activity of novel Pd/TiO2 nanotube catalystsfor methanol electro-oxidation, J. Solid State Chem., 2005, 178,1996-2000.

[30] Zhao Y., He Y., Zhang H., Zhang S., Qu L., Shi G., Dai L., Super-long alignedTiO$_2$/carbon nanotube arrays, Nanotechnology, 2010, 21, 505702 1-7.

[31] Hardcastle F. D., Raman Spectroscopy of Titania (TiO_2) NanotubularWater-Splitting Catalysts, J. Ark. Acad. Sci., 2011, 65, 43-48.

[32] Song H., Qiu X., Li X., Li F., Zhu W., Chen L., TiO_2 nanotubes promotingPt/C catalysts for ethanol electro-oxidation in acidic media, J. Power Sources,2007, 170, 50-54.

[33] Cao T., Li Y., Wang C., Shao C., Liu Y., A Facile in Situ Hydrothermal Method toSrTiO_3/TiO_2 Nanofiber Heterostructures with High PhotocatalyticActivity, Langmuir, 2011, 27, 2946-2952.

[34] Adachi M., Maruta Y., Harada M., Formation of titania nanotubes with highphoto-catalytic activity, Chem. Lett., 2000, 8, 942-944.

[35] Shen L., Zhang X., Li H., Yaun C., Cao G., Design and Tailoring of a ThreeDimensional TiO_2-Graphene-Carbon Nanotube Nanocomposite for Fast LithiumStorage, J. Phy. Chem. Let., 2011, 1, 3096-3101.

[36] Luca D.L., Donato A., Santalgo S., Faggio G., Messina G., Donato N., Neri G.,Hydrogen sensing characteristics of Pt/TiO_2/MWCNTs composites, Int. J. Hydr.Energy, 2012, 37, 1842-1851.

[37] Kang S.H., Jeon T.Y., Kim H.S., Sung Y.E., Smyrl W.H., Effect of Annealing PtNiNanophases on Extended TiO_2 Nanotubes for the Electrochemical OxygenReduction Reaction, J. Electrochem. Soc., 2008, 155, B1058-B1065.

[38] Montero-Ocampo C., Vargas Garcia J.R., Arce Estrada E., Comparison of $TiO_2$and TiO_2-CNT as Cathode Catalyst Supports for ORR, Int. J. Electrochem.Sci., 2013, 8, 12780-12800.

[39] Guo X., Guo D.J., Qiu X.P., Chen L.Q., Zhu W.T., Excellent dispersion andelectrocatalytic properties of Pt nanoparticles supported on novel porous anataseTiO$_2$ nanorods, J. Power Sources, 2009, 194, 281-285.

[40] Dhanasekaran P., Vinod Selvaganesh S., Bhat S.D., Preparation of TiO_2-TiNcomposite nanowires as a support with improved long-term durability in acidicmedium for polymer electrolyte fuel cells, New J. Chem., 2017, 41,2987-2996.

[41] Song H., Qiu X., Li F., Effect of heat treatment on the performance ofTiO2-Pt/CNT catalysts for methanol electro-oxidation, Electrochim. Acta, 2008,53, 3708-3713.

[42] Bedolla-Valdez Z.I., Verde-Gómez Y., Valenzuela-Muñiz A.M., Gochi-PonceY., Oropeza-Guzmán M.T., Gilles Berhault, Alonso-Núñez G.,Sonochemical synthesis and characterization of Pt/CNT, Pt/TiO_2, andPt/CNT/TiO_2 electrocatalysts for methanol electro-oxidation, Electrochim.Acta, 2015, 186, 76–84.

[43] Song H., Qiu X., Li X., Li F., Zhu W., Chen L., TiO_2 nanotubes promotingPt/C catalysts for ethanol electro-oxidation in acidic media, J. PowerSources,2007, 170, 50-54.

[44] Dai L.M., Carbon Nanotechnology: Recent Developments in Chemistry, Physics,Materials Science and Device Applications, 2006, Amsterdam: Elsevier.

[45] Vinod Selvaganesh S., Sridhar P., Pitchumani S., Shukla A.K., Pristine andgraphitized-MWCNTs as durable cathode-catalyst supports for PEFCs, J. Solid StateElectrochem., 2014, 18, 1291-1305.

[46] Selvarani G., Vinod Selvaganesh S., Krishnamurthy S., Kiruthika G.V.M., SridharP., Pitchumani S., Shukla A.K., A Methanol-Tolerant Carbon-Supported Pt-Au AlloyCathode Cat-

alyst for Direct Methanol Fuel Cells and Its Evaluation by DFT, J.Phys Chem C, 2009, 113, 7461-7468.

[47] Fuel Cell Technical Team Roadmap, U.S Department of Energy (USDoE), June 2013.

[48] Santalgo S., Faggio G., Messina G., Fazio E., Neri F., Neri G., On the hydrogensensing mechanism of Pt/TiO_2/CNTs based devices, Sensors and Actuators B:Chemical, 2013, 178, 473-484.

[49] Zhou C., Wang H., Peng F., Liang J., Yu H., Yang J., MnO_2/CNT Supported Ptand PtRu Nanocatalysts for Direct Methanol Fuel Cells, Langmuir, 2009,25, 7711-7717.

[50] Qin Y.H., Li Y., Lv R.L., Wang T.L., Wang W.G., Wang C.W., Enhanced methanoloxidation activity and stability of Pt particles anchored on carbon-doped TiO_2nanocoating support, J. Power Sources, 2015, 278, 639-644.

[51] He X., Hu C., Buiding three-dimensional Pt catalysts on TiO_2 nanorod arraysfor effective ethanol electrooxidation, J. Power Sources, 2011, 196,3119-3123.

[52] Tauster S.J., Fung S.C., Baker R.T.K., Horsley J.A., Strong-interactions insupported-metal catalysts. Science, 1981, 211, 1121-1125.

[53] Eder D., Carbon Nanotube-Inorganic Hybrids. Chem. Rev., 2010, 110,1348-1385.

[54] Kinoshita K., Lundquis J.T., Stonehart P., Potential cycling effects on platinumelectrocatalyst surfaces, Electrochem., 1973, 48, 157-166.

[55] Alliata D., Häring P., Haas O., Kötz R., Siegenthaler H., In Situ AtomicForce Microscopy of Electrochemically Activated Glassy Carbon, Electrochem.Solid-State Lett., 1999, 2, 33-35.

[56] Yi Y., Weinberg G., Prenzel M., Greiner M., Heumann S., Becker S., SchlöglR., Electrochemical corrosion of a glassy carbon electrode, Catal. Today, 2017,295, 32-40.

[57] Vinod Selvaganesh S., Selvarani G., Sridhar P., Pitchumani S., Shukla A. K.,Graphitic Carbon as Durable Cathode-Catalyst Support for PEFCs, Fuel Cells 2011, 11, 372–384.

[58] Kannan R., Pillai V.K., Applications of carbon nanotubes in polymer electrolytemembrane fuel cells, J. Indian Inst. Sci., 2009, 89, 425-436

[59] Xia B.Y., Wang B., Wu H.B., Liu Z., Wang X., Wen X., (David) Lou.,Sandwich-structured TiO_2–Pt–graphene ternary hybrid electrocatalysts withhigh efficiency and stability, J. Mater. Chem., 2012, 22, 16499-16505.

Supplementary Information

Table 1S: Pt mean crystallite size for Pt/MWCNT, Pt/TNW and Pt/TWCNTs before and after AST.

Catalyst	Pt Mean Crystallite size	
	Before AST	After AST
Pt/MWCNT	4.3	7.8
Pt/TNW	3.6	5.1
Pt/TWCNT-1	3.5	–
Pt/TWCNT-2	4.0	6.0
Pt/TWCNT-3	4.8	–

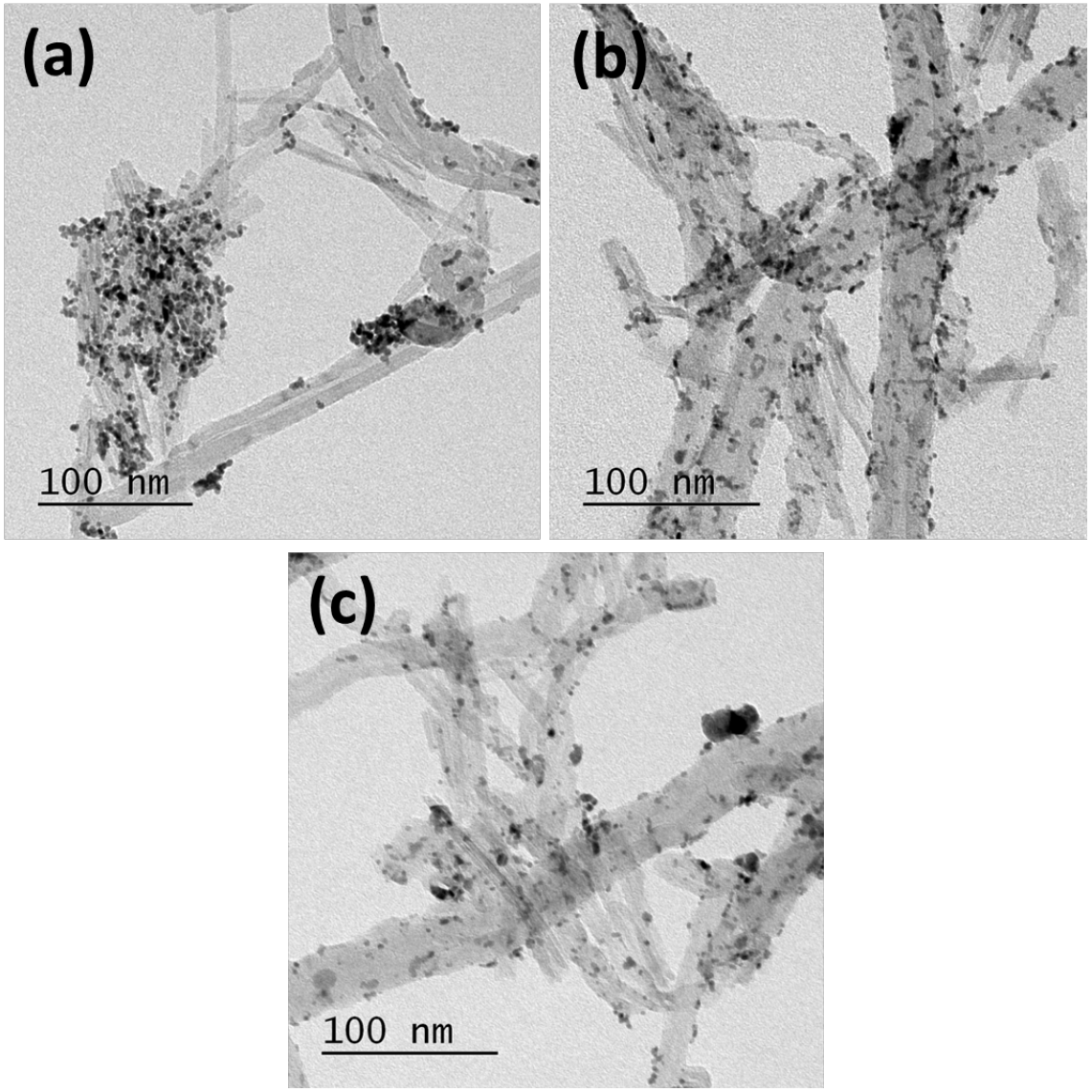

Figure 1S: Comparative HR-TEM micrographs for (a) Pt/TWCNT-1, (b) Pt/TWCNT-2 and (c) Pt/TWCNT-3 nanocomposite.

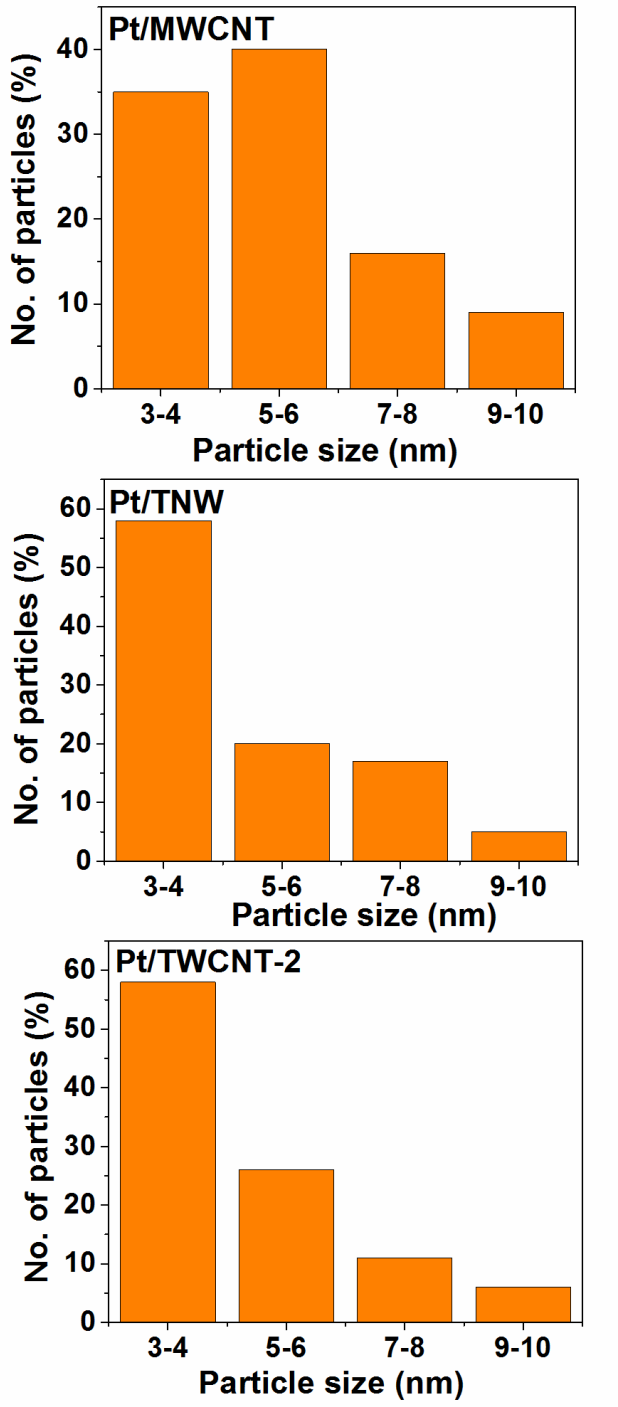

Figure 2S: Histogram showing the Pt particle size distribution for Pt/MWCNT, Pt/TNW and Pt/TWCNT-2.

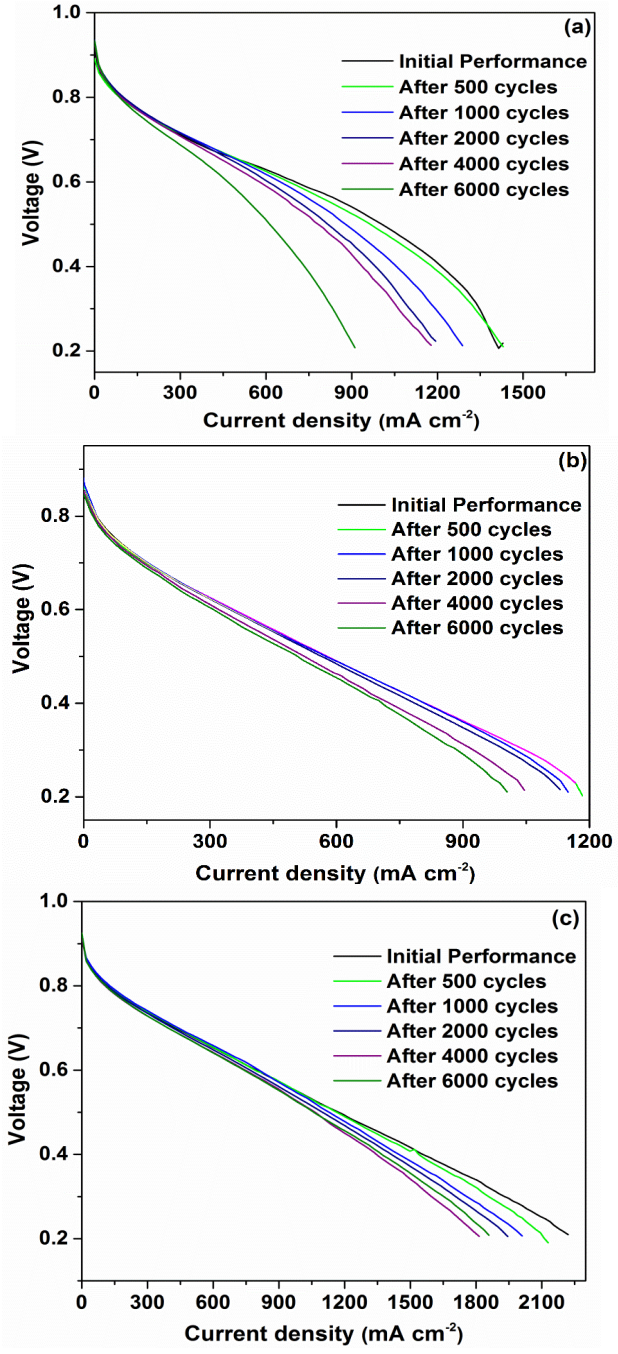

Figure 3S: Comparative polarization plots for PEFCs with Pt/MWCNT, Pt/TNW and Pt/TWCNT electrocatalysts taken before AST and during frequent intervals of AST.

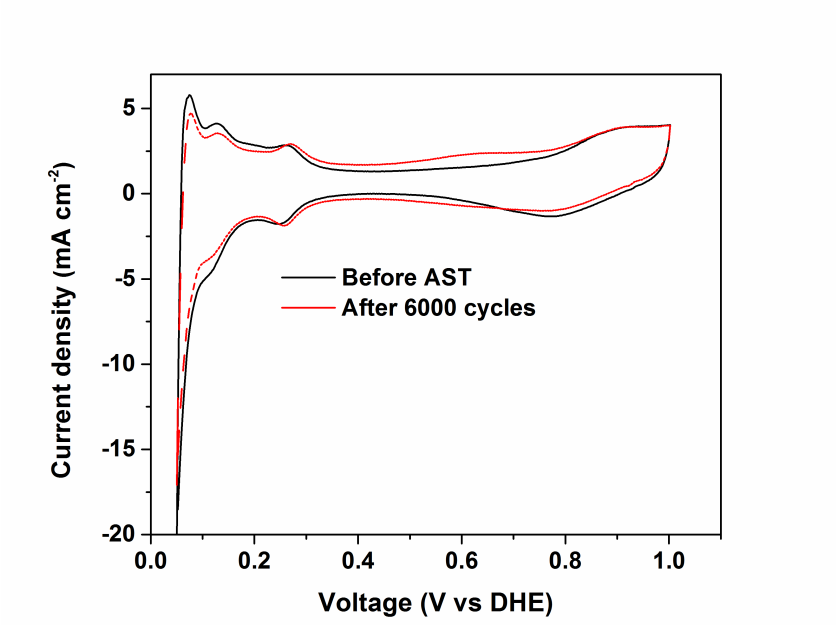

Figure 4S: CV for PEFC with Pt/MWCNT before and after AST.

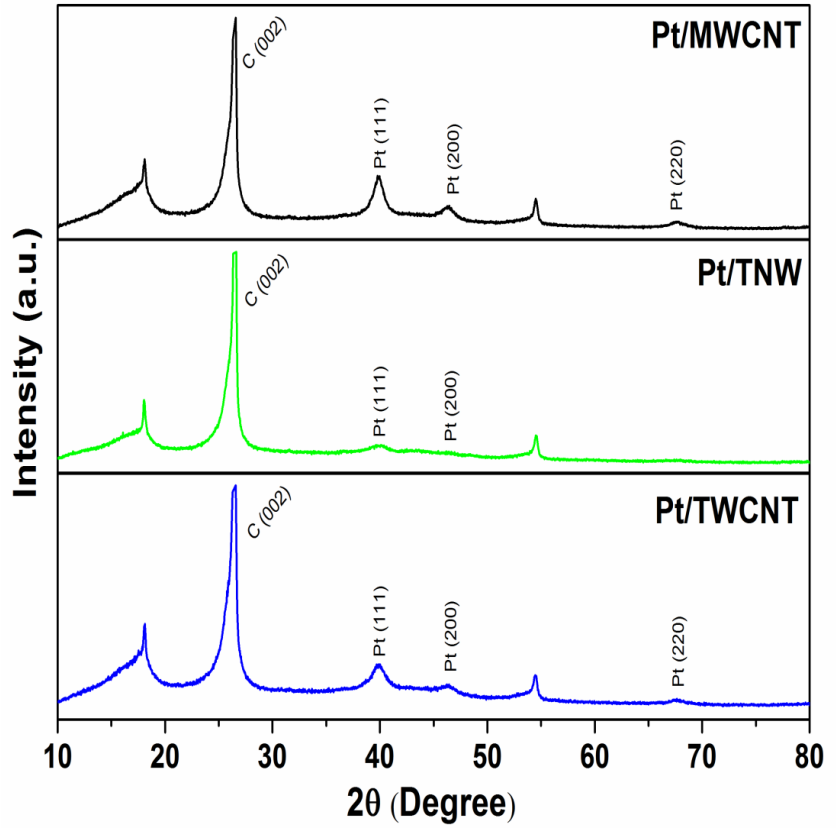

Figure 5S: Powder XRD pattern for Pt/MWCNT, Pt/TNW and Pt/TWCNT electrocatalysts after AST.

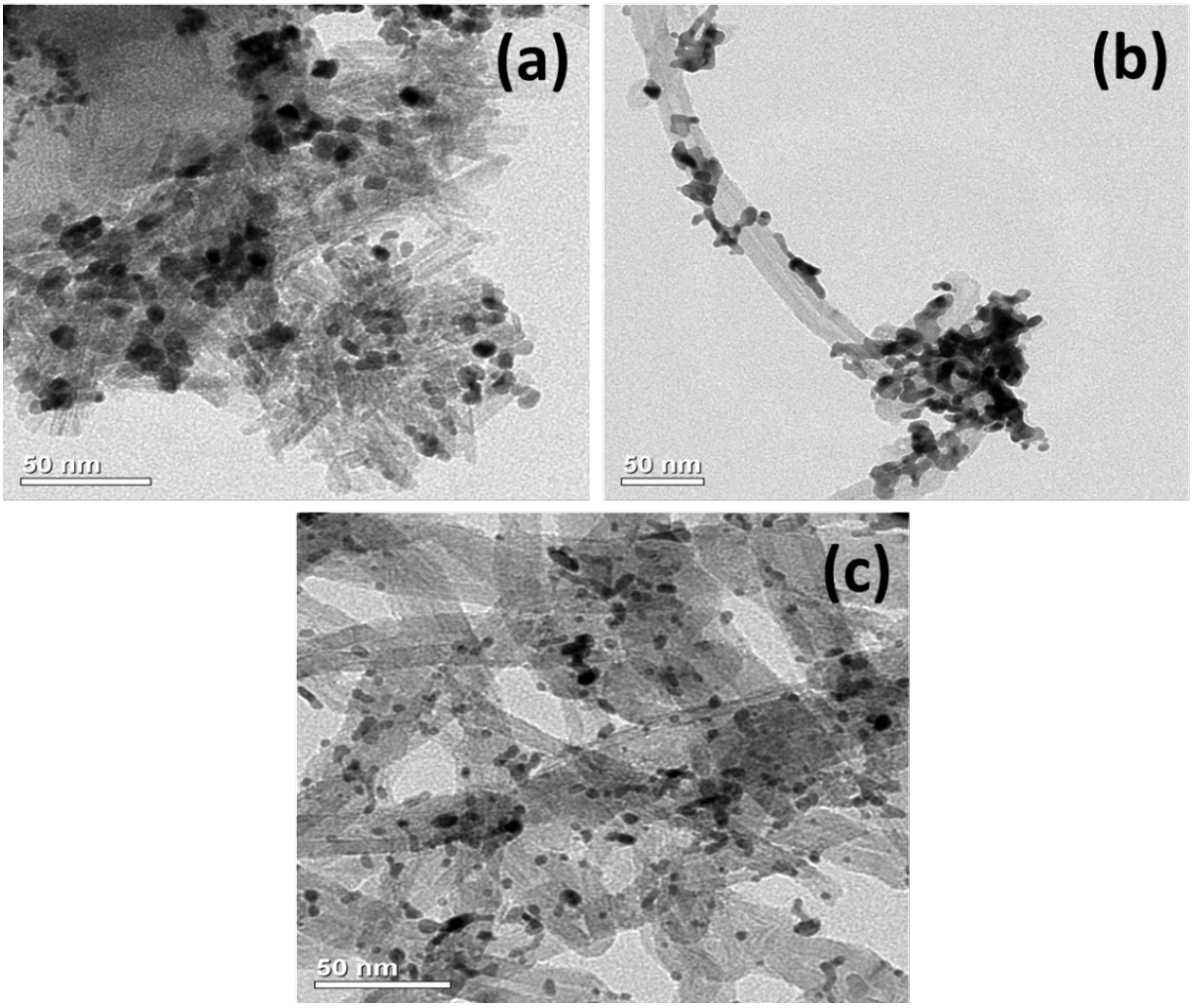

Figure 6S: TEM micrographs for Pt/MWCNT, Pt/TNW and Pt/TWCNT electrocatalysts after AST.